MATERIALS AND METHODS

Chemistry

2-{3-[1-Carboxy-2-(4-fluoro-benzylsulfanyl)-ethyl]-ureido}-pentanedioic acid (DCFBC). (**Supplemental Figure 1**) To a solution of 43 mg (0.146 mmoles) 2-[3-(1-carboxy-2-mercapto-ethyl)-ureido]-pentanedioic acid (**1**) dissolved in 100 µL water was added 38 mg 4-fluorobenzyl bromide in 400 µL methanol. To this was added 50 mg (0.6 mmoles) ammonium bicarbonate. The reaction mixture was heated for 10 min at 50^{o}C, then cooled and diluted with 300 µL of acetonitrile and 200 µL trifluoroacetic acid, concentrated, and dried under vacuum. The residue was dissolved in 1 mL water and a few drops of acetonitrile. The solution was then loaded onto an activated Waters C18 Sep-Pak and eluted with 25 mL water, 25 mL water containing 0.1% trifluoroacetic acid, followed by 50 mL of 90% water/10% acetonitrile containing 0.1% trifluoroacetic acid, and finally with 50 mL of 80% water/20% acetonitrile containing 0.1% trifluoroacetic acid. Fractions were analyzed by reverse phase C18 thin layer chromatography (Merck HPTLC silica gel 60RP-18 $WF_{254}S$ plates using 75% water/25% acetonitrile containing 0.1% TFA). Product R_f = 0.25. Plates were visualized in an iodine chamber. Product was further purified by semi-preparative high-performance liquid chromatography (HPLC, 10 x 250 mm Atlantis T3, 5µ, C18 column, mobile phase 70% water/30% acetonitrile containing 0.1% trifluoroacetic acid, flow rate 4 mL/min). Product eluted at 11.5 min. Material was collected, concentrated, and dried under vacuum to give 16 mg product in 27% overall yield. ^{1}H-NMR (1/1 D_2O/CD_3CN) δ7.38 (dd, J = 8.4, 5.2Hz, 2H), 7.14 (t, J = 8.8Hz, 2H), 4.44 (dd, J = 7.2, 5.2Hz, 1H), 4.29 (dd, J = 8.8, 4.8Hz, 1H), 3.81 (s, 2H), 2.90 (m, 2H), 2.50 (t, J = 7.6 Hz, 2H), 2.17 (m, 1H), 1.98 (m, 1H). $[\alpha]^{23}_{D}$ -24.2 (c 0.0031, MeOH). ESI-MS Calcd. for $C_{16}H_{20}FN_2O_7S$ $[M + H]^+$ 403.1, found 402.9. Anal. Calcd. For $C_{16}H_{19}FN_2O_7S{\cdot}H_2O$, 420.4099, C 45.71, H 5.03, N 6.66, S 7.63. Found C 45.54, H 4.80, N 6.67, S 7.50.

Radiochemistry

2-{3-[1-Carboxy-2-(4-[^{18}F]fluoro-benzylsulfanyl)-ethyl]-ureido}-pentanedioic acid, ^{18}F-DCFBC.

(**Supplemental Figure 1**) Reagents, solvents, and reaction intermediates were added, transferred or injected by positive pressure or through the use of model XLP 6000 Cavrol pumps (Tecan Group, Ltd., San Jose, CA). The microwave is fitted with a custom cavity that allows cooling. Following purification by HPLC, ^{18}F-DCFBC was concentrated and reformulated using an automated solid phase extraction (SPE) system consisting of three syringe pumps and switching valves. The microwave radiochemistry and SPE systems are controlled with a laptop computer using LabView™ software and a compact FieldPoint Controller (National Instruments, Austin, TX).

^{18}F-KF was produced by 18 MeV proton bombardment of a high pressure ^{18}O-H_2O target using a General Electric PETtrace biomedical cyclotron (GE HealthCare, Waukesha, WI). The irradiated target water was passed through a Chromafix 30-PS-HCO3 QMA cartridge to trap the ^{18}F-fluoride. The cartridge was eluted with 0.15 mL of a 1:1 solution of acetonitrile:water containing 2.3 mg potassium carbonate and 12 mg kryptofix 2.2.2 into a 5 mL Wheaton reaction vial followed by a 0.25 mL acetonitrile rinse of the cartridge. The ^{18}F-Fluoride and potassium carbonate were azeotropically dried with multiple additions of acetonitrile at 100˚C under a nitrogen flow and vacuum. A solution of 4-formyl-*N*,*N*,*N*-trimethylanilinium triflate (4 mg in 0.4 mL acetonitrile) was added to the reaction vessel followed by irradiation at 50W for 30 sec. Next an aqueous solution of sodium borohydride (1.2 mg in 0.2 mL water) was added and the vessel was further irradiated at 50W for 30 sec. Next 0.8 mL of hydrobromic acid, 48% in water by weight, was added and the vessel was further irradiated at 25W for 180 sec. The reaction mixture was eluted through a Waters Oasis HLB Plus cartridge (Waters Corp., Milford, MA). The reaction vial was rinsed with 1 mL HPLC-grade water, with the rinsing passed through the Waters Oasis

HLB Plus cartridge. The Oasis HLB Plus Cartridge was washed with an additional 12 mL of HPLC-grade water, flushed with 12 mL air, followed by elution of 4-^{18}F-fluorobenzyl bromide with 1 mL of acetonitrile into a second reaction vessel containing 0.6 mg **1** and 100 μL tetrabutylammonium hydroxide (1 M in water). The reaction mixture was allowed to stand for 10 min at room temperature followed by acidification with 3.5 mL of 0.5 M o-phosphoric acid, filtration through a 0.45 μm Teflon™ filter, and injection into the semi-preparative HPLC for purification using a semi-preparative Waters Atlantis T3 reverse phase C_{18} 5μ 250 x 10 mm column and a 20% acetonitrile:80% triethylamine/phosphate buffer (pH 3.2) mobile phase at a flow rate of 8 mL/minute. ^{18}F-DCFBC elutes at 22 min. The ^{18}F-DCFBC fraction was collected in 50 mL water containing 0.25 g ascorbic acid. The water reservoir was pressurized to load the ^{18}F-DCFBC onto a Waters Oasis HLB solid phase extraction cartridge. The Oasis HLB was then washed with 10 mL 0.9% sodium chloride. ^{18}F-DCFBC was eluted from the Oasis HLB Plus cartridge (Waters Corp., Milford, MA) with 1 mL of ethanol followed by 10 mL of 0.9% sodium chloride (American Regent, Shirley, NY, 10 mL single dose in glass) via a sterilizing 0.22 μm filter into a sterile vial containing 4 mL 0.9% sodium chloride (American Regent, 10mL single dose in glass).

Chemical purity and radiochemical purity was measured by injection of 50μL of the final preparation of ^{18}F-DCFBC onto a radio-HPLC using a 4.6 X 100mm Waters Atlantis T3, 5 micron, C18 column with a mobile phase of 30% acetonitrile:70% triethylamine/phosphate buffer pH 3.2 at a flow rate of 1mL/min and UV detection at 220nM. The mass corresponding to ^{18}F-DCFBC was determined from the area under the UV peak of ^{18}F-DCFBC and a standard curve of DCFBC previously prepared on this radio-HPLC system. This was used to calculate the specific activity of the preparation. Chemical identity of the tracer was

confirmed by radio-HPLC analysis of 50μL of the final preparation of ^{18}F-DCFBC that had been spiked with authentic DCFBC.

Dosimetry Methods

By default OLINDA/EXM assumes that the TIACs assigned to GI tract organs were in the contents and not in the wall. In the case of ^{18}F-DCFBC, there is no activity within the contents and all organ self-dose reflects wall-to-wall emissions. The dose estimates from OLINDA/EXM for the GI tract walls were corrected to account for the difference in emission source assuming self-absorption of β emissions as described by Stabin (*20*).

Estimates for the red marrow activity coefficients were obtained using ROIs drawn on both the femoral heads and the spine. The time integrated activity coefficient for red marrow estimated from the femoral head ROI was selected for subsequent dose calculations as it was larger and would represent a conservative estimate, and this larger value was used for the calculation of the remainder of body dose.

Determination of the integrated time activity coefficient for the urinary bladder contents requires selection of an appropriate voiding period. **Supplemental Figure 5** shows the effect of voiding period on the integrated time activity coefficient for the bladder contents using the voiding model of Cloutier et. al (*24*). A voiding time of one hour was selected as patients with treated prostate cancer can have difficulty maintaining continence, and it is expected that patients would void prior to imaging in general clinical practice.

Renal excretion was assumed to be the sole route of elimination for ^{18}F-DCFBC as there was no appreciable concentration in the gallbladder during the time of acquisition to suggest hepatic excretion. Excreted radiotracer was accounted for through ROI contours drawn on the bladder contents. In the case where patients voided between the 4th and 5th PET acquisitions, the excreted activity was accounted for by the difference in decay-corrected total activity in the PET field-of-view (FOV), which is expected to remain constant in the setting of no excretion.

The dose to the bladder wall is dependent upon the amount of radiotracer used, decay energy characteristics, physical decay constant (λ_p), biological excretion or decay constant (λ_b), and the voiding interval. The biological decay constant was determined through fitting the decay-corrected bladder and excretion activities described above to a nonlinear one-phase association model using GraphPad Prism 5 (GraphPad Software, Inc. La Jolla, CA). The model (Equation 1) is shown below and assumes 100% urinary excretion of the injected radiotracer.

$$\frac{A_{excreted}}{A_{injected}} = \left(1 - e^{-\lambda_b t}\right) \quad (1)$$

The time-integrated activity coefficient for the urinary bladder wall was calculated using the voiding model of Cloutier (Equation 2) which is included in OLINDA/EXM (*21*).

$$N_{bladder} = A_{injected} \sum_i f_i \left[\frac{1-e^{-\lambda_p T}}{\lambda_p} - \frac{1-e^{-(\lambda_b+\lambda_p)T}}{\lambda_b+\lambda_p}\right]\left[\frac{1}{1-e^{-(\lambda_b+\lambda_p)T}}\right] \quad (2)$$

In the above equation, $N_{bladder}$ represents the total area under the time-activity curve for the bladder (Bq-h), f_i the fraction of activity excreted for a given biological excretion constant (assumed to be unity

for the case of the current analysis), and T represents the voiding time (h). Dividing the above result by the injected activity leads to the time-integrated activity coefficient for the bladder (Bq-h/ Bq).

Human Serum Derived PSMA assay

An *in vitro N*-acetylaspartylglutamate (NAAG) hydrolysis assay was utilized as previously described (*23*). DCFBC was used at log-unit final concentrations that ranged from 100 μM to 100 fM to assess hydrolysis of ^{3}H-NAAG in normal human serum-derived PSMA enzymatic activity to calculate the percentage of enzyme inhibition and determine the 50% inhibitory concentration (IC_{50}) for DCFBC.

Whole Blood and Plasma Activity

Patient whole blood was collected in EDTA tubes at the following times after administration of ^{18}F-DCFBC after PET2, PET4 and PET5 (approximately 24, 88, and 152 minutes post-injection when averaging about 8 FOV per PET series). Samples were collected for patients 2 through 5. Whole blood and plasma was counted on a gamma counter with decay correction and calculated for cpm per mL of whole blood or plasma. Patient hematocrit from the day post-injection follow-up visit was used to derive an inverse plasmacrit (1 – percent hematocrit) to derive plasma activity present in 1 mL of whole blood.

RESULTS

Human GCPII Inhibition by DCFBC

In order to determine whether DCFBC could inhibit a circulating form of PSMA that may be present in human blood, which might account for persistent blood pool radioactivity, we tested the inhibitory

capacity of DCFBC in a sample of normal human plasma. DCFBC inhibited NAAG hydrolysis in normal human plasma with a calculated IC_{50} of 3 nM (**Supplemental Figure 6**). Other compounds of the urea class of PSMA inhibitors demonstrated inhibition at similar or higher levels of potency, including 2-(3-{1-carboxy-5-[(6-fluoro-pyridine-3-carbonyl)-amino]pentyl}-ureido)pentanedioic acid (DCFPyL) and Trofex™ (data not shown).

Supplemental Table 1. Patient Specific Data.

	Age	Weight (kg)	Height (m)	BMI	Dose (MBq)
DCFBC-01	56	83	1.7	28.72	372.96
DCFBC-02	79	100	1.9	27.70	360.01
DCFBC-03	74	82	1.65	30.12	360.38
DCFBC-04	59	108	1.88	30.56	359.27
DCFBC-05	62	92	1.88	26.03	378.51
Average	66.0	93.0	1.8	28.6	366.2
Std Dev	10.0	11.1	0.1	1.8	8.9

Supplemental Table 2. Clinical Imaging Data – Patient clinical, ^{18}F-DCFBC-PET/CT, and correlative CT and bone scan interpretation.

Patient	PSA (ng/mL)	GS[§]	Treatment History	Lesion	Site	Location	^{18}F-DCFBC PET Tumor Uptake				PET and CIM Interpretations		
							SUVmax	T/L	T/BP	T/M	PET	CT	BS
1	9.5	9	Prostatectomy, Hormone Refractory (Lupron)	1	LN	Aortic bifurcation	6.5	1.97	1.97	13.00	Pos	Neg	N/A*
				2	Bone	T12	4.7	1.42	1.42	9.40	Pos	Pos	Pos
				3	Bone	L4	3.4	1.03	1.03	6.80	Pos	Neg	Neg
				4	Bone	Left post. iliac	3.3	1.00	1.00	6.60	Pos	Neg	Pos
				5	Bone	Left iliac wing	3.6	1.09	1.09	7.20	Pos	Neg	Pos
				6	Bone	Left sacrum (SI)	3.0	0.91	0.91	6.00	Pos	Neg	Neg
				7	Bone	Right sacrum	5.4	1.64	1.64	10.80	Pos	Neg	Neg
				8	Bone	Left iliac	5.7	1.73	1.73	11.40	Pos	Neg	Neg
				9	Bone	Lower sacrum	4.4	1.33	1.33	8.80	Pos	Pos	Pos
				10	Bone	Right ischium	8.2	2.48	2.48	16.40	Pos	Neg	Pos
				11	Bone	Left ischium	2.8	0.85	0.85	5.60	Pos	Neg	Neg
				12	Bone	Left acetabulum	2.7	0.82	0.82	5.40	Pos	Neg	Neg
				13	Bone	Right ant. 3rd rib	1.4	0.42	0.42	2.80	Neg	Neg	Pos
2	14.8	7	Prostatectomy, Hormone Refractory (Ketaconazole)	1	LN	Portocaval	5.2	1.93	1.73	8.67	Pos	Pos	N/A*
				2	LN	Aortocaval	6.2	2.30	2.07	10.33	Pos	Pos	N/A*
				3	LN	Pre-Aortic	6.8	2.52	2.27	11.33	Pos	Pos	N/A*
				4	LN	Right aortocaval	5.2	1.93	1.73	8.67	Pos	Pos	N/A*
				5	LN	Right Aortocaval	5.8	2.15	1.93	9.67	Pos	Pos	N/A*
				6	Bone	Right post. iliac	4.0	1.48	1.33	6.67	Pos	Neg	Neg
				7	LN	Right com. iliac	5.6	2.07	1.87	9.33	Pos	Pos	N/A*
				8	LN	Left com. iliac	4.3	1.59	1.43	7.17	Pos	Pos	N/A*
				9	LN	Left ext. iliac	7.7	2.85	2.57	12.83	Pos	Pos	N/A*
				10	Bone	L3	5.6	2.07	1.87	9.33	Pos	Neg	Neg
				11	Bone	Right rib 9	1.6	0.59	0.53	2.67	Neg	Neg	Pos*
				12	Bone	Left rib 5	0.9	0.33	0.30	1.50	Neg	Neg	Pos*
				13	Bone	Left rib 6	1.6	0.59	0.53	2.67	Neg	Neg	Pos*
				14	Bone	Left rib 7	1.3	0.4	0.4	2.17	Neg	Neg	Pos*

								8	3				
3	9.4	7	Brachytherapy and pelvic	1	Bone	T12	2.7	1.08	5.40	1.23	Pos	Neg	Neg
			XRT, Started Hormone	2	Bone	L3	2.6	1.04	5.20	1.18	Pos	Neg	Neg
			Therapy 16 days prior to PET	3	Bone	Right post. iliac	1.1	0.44	2.20	0.50	Neg	Pos	Pos
4	26.6	9	prostatectomy,	1	LN	Left paraaortic	2.3	1.00	0.88	4.60	Pos	Pos	N/A*
			Pelvic XRT	2	LN	Left com. iliac	3.0	1.30	1.15	6.00	Pos	Pos	N/A*
			Valproic Acid	3	LN	Left ext. iliac	4.1	1.78	1.58	8.20	Pos	Pos	N/A*
				4	Bone	Left 10th rib	N/A	N/A	N/A	N/A	Neg	Neg	Pos#
				5	Bone	Right T7	N/A	N/A	N/A	N/A	Neg	Neg	Pos#
5	46.5	9	Prostatectomy,	1	LN	Left paraaortic	5.3	1.56	1.77	10.60	Pos	Pos	N/A*
			Discontinued Valproic	2	LN	Right com. iliac	9.8	2.88	3.27	19.60	Pos	Pos	N/A*
			Acid	3	LN	Right com. iliac	5.7	1.68	1.90	11.40	Pos	Pos	N/A*
				4	LN	Right ext. iliac	11.6	3.41	3.87	23.20	Pos	Pos	N/A*
				5	LN	Left ext. iliac	5.3	1.56	1.77	10.60	Pos	Pos	N/A*
				6	Bone	Left post. rib 11	N/A	N/A	N/A	N/A	Neg	Neg	Pos*
				7	Bone	Left acetabulum	N/A	N/A	N/A	N/A	Neg	Pos	Neg
				8	Bone	L3	N/A	N/A	N/A	N/A	Neg	Pos	Neg

* - Chronic change

\# - Degenerative or fracture

N/A - very low level PET uptake - SUV not measured

N/A* - lymph node assessment not applicable in bone scintigraphy

§ - maximum Gleason Score at time of initial diagnosis

Pos = positive for metastatic disease;

Neg = Negative for metastatic disease

T/L = Tumor SUV_{max}/Liver SUV_{avg}

T/BP = Tumor SUV_{max}/Blood Pool SUV_{avg}

T/M = Tumor SUV_{max}/Muscle SUV_{avg}

Supplemental Table 3. Individual Patient – Time-Integrated activity coefficients (Bq-h/Bq)

	DCFBC-01	DCFBC-02	DCFBC-03	DCFBC-04	DCFBC-05		Average	Std Dev	COV
Adrenals	1.30E-03	8.89E-04	8.81E-04	9.21E-04	6.42E-04		9.26E-04	2.35E-04	25.43 %
Brain	1.42E-02	1.21E-02	1.17E-02	1.13E-02	1.09E-02		1.20E-02	1.30E-03	10.78 %
GB Contents	3.57E-03	2.38E-03	2.07E-03	2.68E-03	1.79E-03		2.50E-03	6.87E-04	27.47 %
LLI Contents	2.10E-02	1.22E-02	1.12E-02	1.30E-02	1.26E-02		1.40E-02	3.96E-03	28.29 %
SI Contents	5.28E-02	5.62E-02	4.72E-02	4.77E-02	4.25E-02		4.93E-02	5.35E-03	10.85 %
Stomach	2.47E-02	1.69E-02	2.00E-02	1.89E-02	1.78E-02		1.96E-02	3.06E-03	15.55 %
ULI Contents	1.82E-02	1.53E-02	1.43E-02	1.67E-02	1.15E-02		1.52E-02	2.55E-03	16.76 %
Heart Contents	6.03E-02	4.59E-02	4.27E-02	4.72E-02	4.28E-02		4.78E-02	7.26E-03	15.20 %
Heart Wall	2.52E-02	2.02E-02	2.11E-02	2.04E-02	1.81E-02		2.10E-02	2.58E-03	12.31 %
Kidneys	4.27E-02	3.50E-02	2.93E-02	3.86E-02	2.94E-02		3.50E-02	5.84E-03	16.68 %
Liver	2.08E-01	1.38E-01	1.66E-01	1.62E-01	1.22E-01		1.59E-01	3.29E-02	20.62 %
Lungs	1.10E-01	7.99E-02	1.11E-01	1.32E-01	1.11E-01		1.09E-01	1.87E-02	17.13 %
Pancreas	6.16E-03	5.78E-03	5.47E-03	5.46E-03	3.83E-03		5.34E-03	8.93E-04	16.73 %
Spleen	1.11E-02	8.89E-03	1.09E-02	9.97E-03	9.81E-03		1.01E-02	8.92E-04	8.80%
Testes	2.70E-03	1.51E-03	1.38E-03	2.68E-03	3.83E-03		2.42E-03	1.00E-03	41.50 %
Thyroid	9.09E-04	7.85E-04	7.71E-04	8.44E-04	6.89E-04		8.00E-04	8.23E-05	10.29 %
Bladder	6.59E-02	1.97E-01	9.67E-02	1.30E-01	1.42E-01		1.26E-01	4.94E	39.13

Contents								-02	%
Red Marrow (Femoral Head)	1.11E-01	1.05E-01	1.24E-01	1.02E-01	9.54E-02		1.08E-01	1.06E-02	9.86%
Red Marrow (Spine)	7.69E-02	7.65E-02	6.16E-02	6.99E-02	6.11E-02		6.92E-02	7.70E-03	11.12 %
Total Body	2.47E+00	2.46E+00	2.38E+00	2.28E+00	2.28E+00		2.37E+00	9.09E-02	3.83%
Remainder of Body	1.73E+00	1.87E+00	1.72E+00	1.59E+00	1.68E+00		1.72E+00	1.01E-01	5.86%

Supplemental Table 4. Individual Patient - Dose in mSv/ MBq administered activity.

	DCFBC-01	DCFBC-02	DCFBC-03	DCFBC-04	DCFBC-05		Average	StdDev	COV
Adrenals	2.29E-02	1.81E-02	1.81E-02	1.82E-02	1.50E-02		1.85E-02	2.83E-03	15.32%
Brain	4.61E-03	4.37E-03	4.19E-03	3.94E-03	3.96E-03		4.21E-03	2.83E-04	6.73%
Breasts	8.81E-03	8.84E-03	8.53E-03	8.14E-03	8.23E-03		8.51E-03	3.22E-04	3.78%
GB Wall	2.09E-02	1.79E-02	1.73E-02	1.77E-02	1.55E-02		1.79E-02	1.95E-03	10.90%
LLI Wall	3.13E-02	2.37E-02	2.22E-02	2.33E-02	2.33E-02		2.47E-02	3.69E-03	14.92%
SI Wall	2.49E-02	2.58E-02	2.30E-02	2.27E-02	2.15E-02		2.36E-02	1.72E-03	7.31%
Stomach Wall	3.57E-02	2.80E-02	3.05E-02	2.90E-02	2.79E-02		3.02E-02	3.24E-03	10.72%
ULI Wall	2.60E-02	2.43E-02	2.28E-02	2.38E-02	2.01E-02		2.34E-02	2.20E-03	9.39%
Heart Wall	3.47E-02	2.82E-02	2.82E-02	2.87E-02	2.61E-02		2.92E-02	3.24E-03	11.12%
Kidneys	3.36E-02	2.85E-02	2.50E-02	3.03E-02	2.44E-02		2.84E-02	3.81E-03	13.45%
Liver	3.09E-02	2.22E-02	2.54E-02	2.49E-02	1.98E-02		2.46E-02	4.16E-03	16.88%
Lungs	2.53E-02	1.98E-02	2.49E-02	2.81E-02	2.44E-02		2.45E-02	2.99E-03	12.22%
Muscle	9.93E-03	1.02E-02	9.71E-03	9.20E-03	9.42E-03		9.69E-03	3.97E-04	4.10%
Ovaries	1.35E-02	1.39E-02	1.31E-02	1.26E-02	1.28E-02		1.32E-02	5.26E-04	3.99%
Pancreas	2.17E-02	2.00E-02	1.95E-02	1.92E-02	1.58E-02		1.92E-02	2.15E-03	11.19%
Red Marrow	1.76E-02	1.72E-02	1.81E-02	1.61E-02	1.58E-02		1.70E-02	9.81E-04	5.79%
Osteogenic Cells	1.86E-02	1.91E-02	1.88E-02	1.71E-02	1.74E-02		1.82E-02	8.92E-04	4.90%
Skin	7.44E-03	7.78E-03	7.31E-03	6.85E-03	7.11E-03		7.30E-03	3.50E-04	4.79%
Spleen	1.86E-02	1.61E-02	1.80E-02	1.69E-02	1.65E-02		1.72E-02	1.05E-03	6.08%
Testes	1.65E-02	1.18E-02	1.10E-02	1.63E-02	2.14E-02		1.54E-02	4.19E-03	27.23%

Thymus	1.15E-02	1.14E-02	1.10E-02	1.05E-02	1.06E-02		1.10E-02	4.53E-04	4.12%
Thyroid	1.26E-02	1.19E-02	1.15E-02	1.17E-02	1.07E-02		1.17E-02	6.87E-04	5.88%
Bladder Wall	2.44E-02	2.63E-02	3.18E-02	3.95E-02	4.00E-02		3.24E-02	7.24E-03	22.35%
Uterus	1.33E-02	1.39E-02	1.34E-02	1.31E-02	1.34E-02		1.34E-02	2.95E-04	2.20%
Total Body	1.14E-02	1.13E-02	1.10E-02	1.05E-02	1.05E-02		1.09E-02	4.28E-04	3.91%
ED	2.18E-02	1.83E-02	1.91E-02	2.02E-02	2.02E-02		1.99E-02	1.34E-03	6.73%

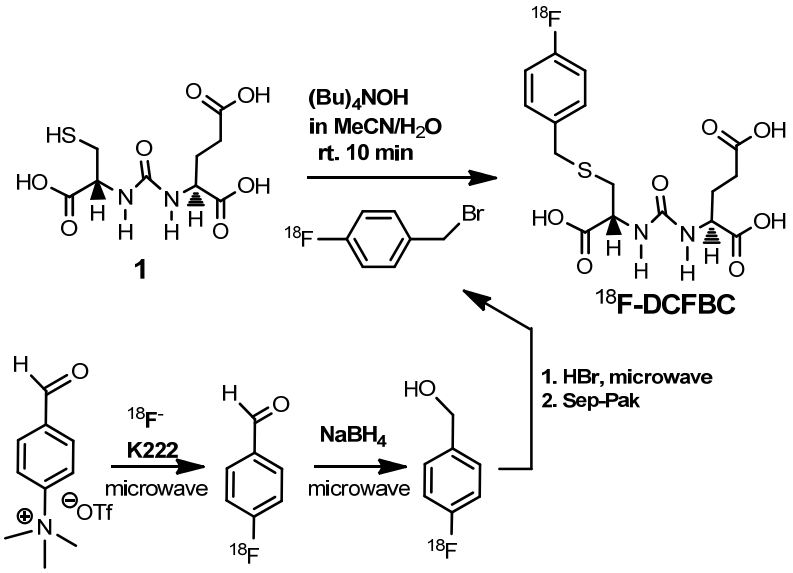

Supplemental Figure 1. ^{18}F-DCFBC Radiochemistry Schema

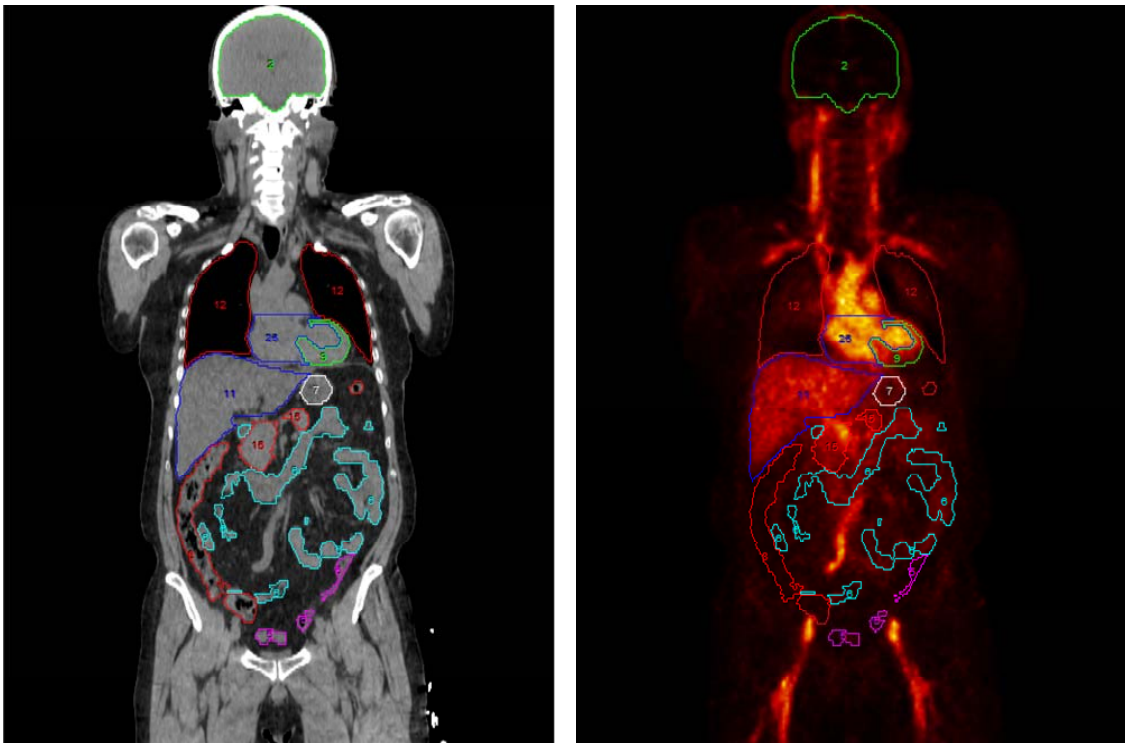

Supplemental Figure 2. Representative organ ROIs shown on CT (left) and PET (right) images. Note the vascular activity and absence of penetration into the brain parenchyma. The scans extend from the skull vertex through the mid-thigh.

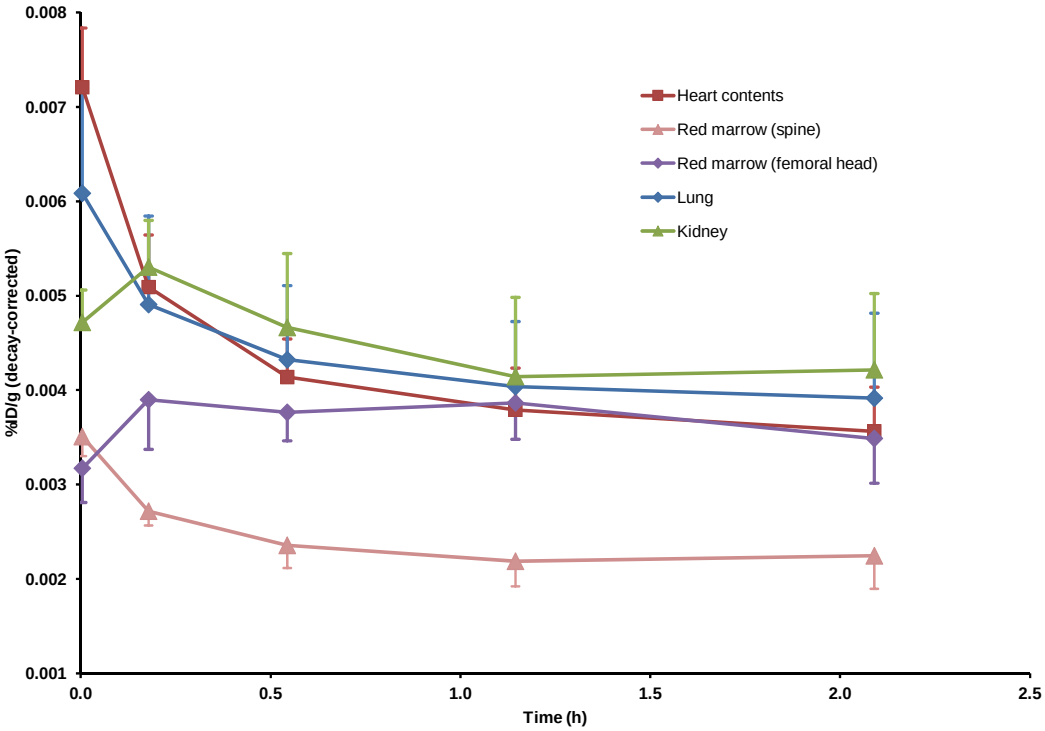

Supplemental Figure 3. Mean biodistribution curves plotted for decay-corrected %ID/g (percent injected dose per gram organ mass) versus time. The time axis represents an average time over all patients for each PET scan as some patients (i.e., tall patients) required more bed positions. Red marrow using data from both the femoral heads and vertebrae with comparison organs as a surrogate for the blood pool concentration.

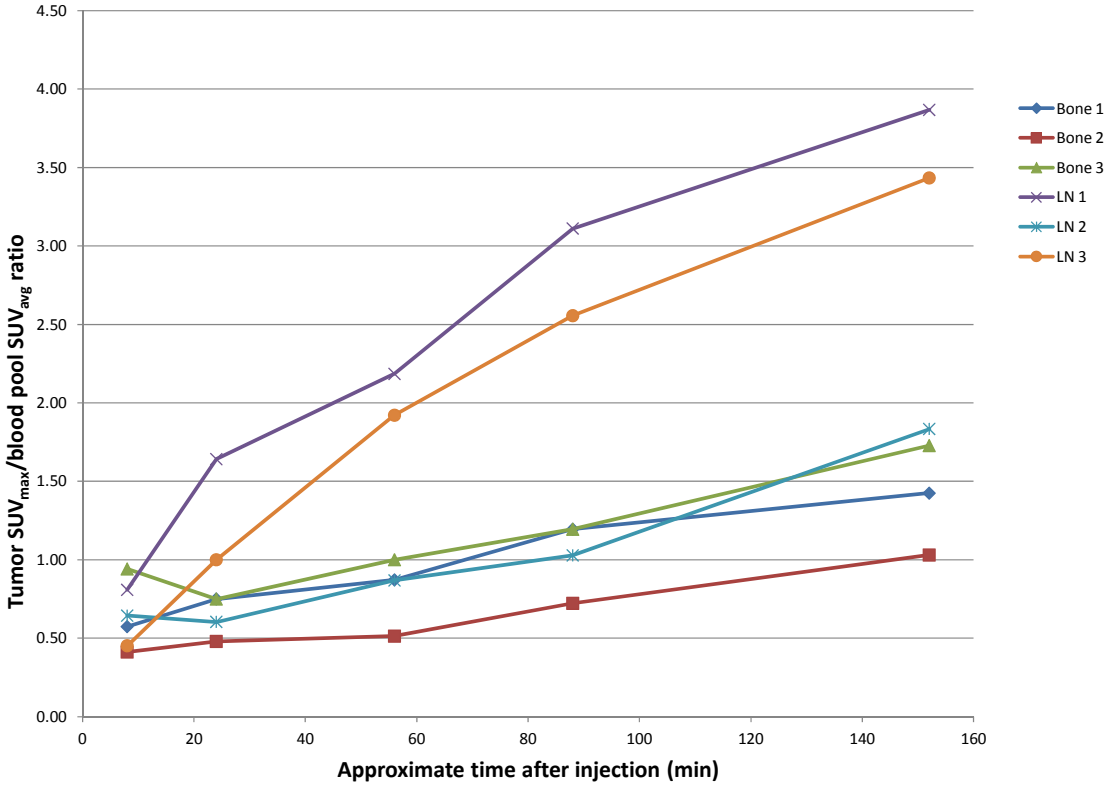

Supplemental Figure 4. Time-activity-curve of selected ^{18}F-DCFBC-PET positive metastatic sites in lymph nodes and bone over serial PET scans up to PET5 (2 h post-injection) normalized to blood pool (tumor SUV_{max}/blood pool SUV_{avg}). Time is plotted as approximate time of completion of post PET series with average of 8 FOV per patient on serial PET imaging as described in PET protocol methods.

A

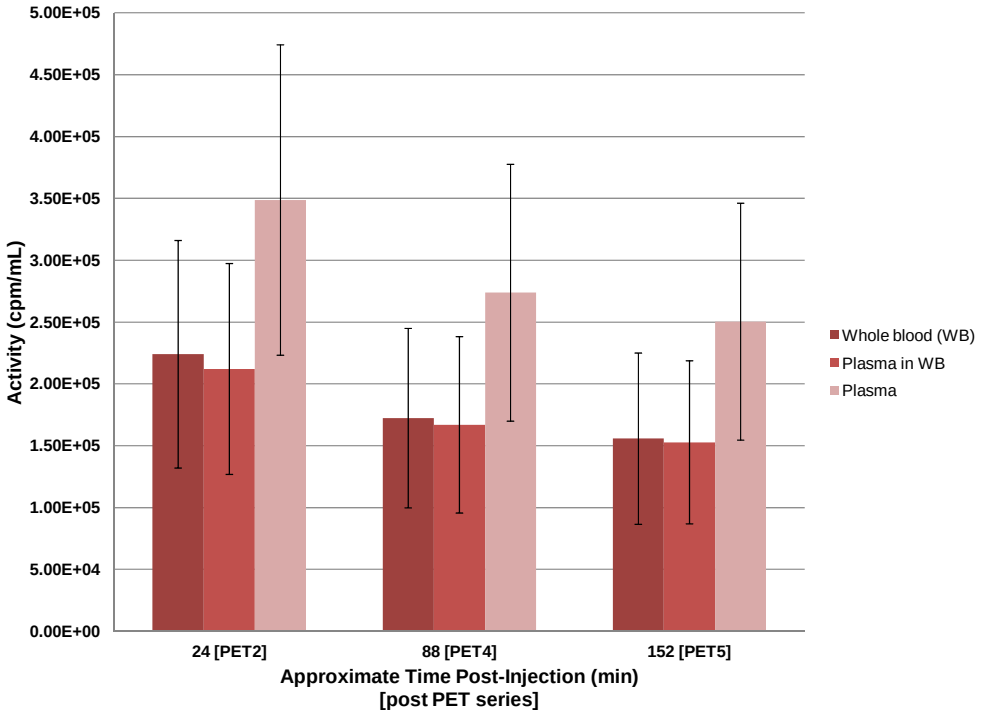
5.00E+05
4.50E+05
4.00E+05
3.50E+05
3.00E+05
2.50E+05
2.00E+05
1.50E+05
1.00E+05
5.00E+04
0.00E+00
Activity (cpm/mL)
24 [PET2]
88 [PET4]
152 [PET5]
Approximate Time Post-Injection (min)
[post PET series]
Whole blood (WB)
Plasma in WB
Plasma

B

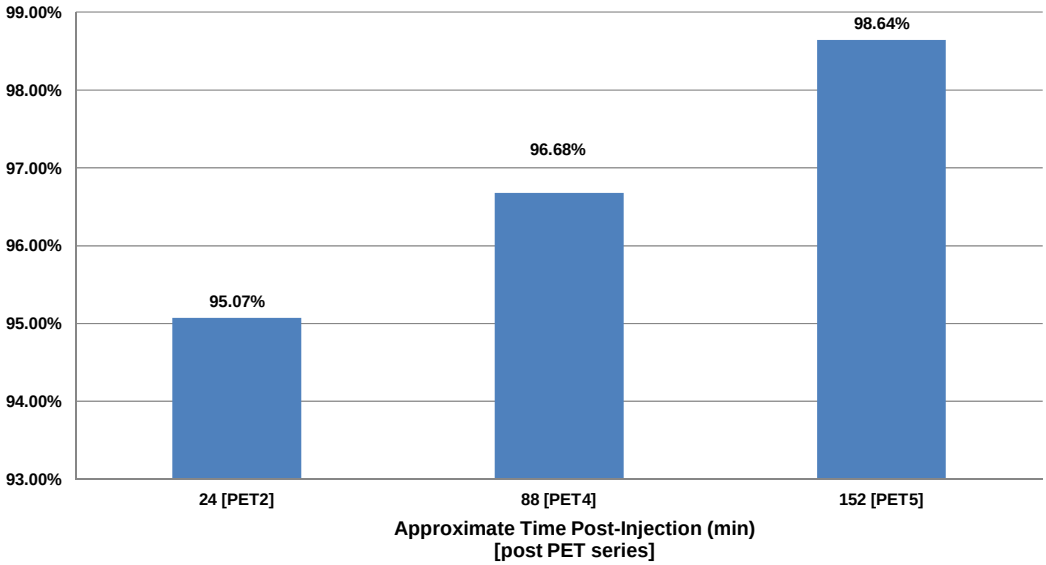
99.00%
98.00%
97.00%
96.00%
95.00%
94.00%
93.00%
95.07%
96.68%
98.64%
24 [PET2]
88 [PET4]
152 [PET5]
Approximate Time Post-Injection (min)
[post PET series]

Supplemental Figure 5. (A) Average activity of ^{18}F-DCFBC (cpm/mL) in patient whole blood, plasma percent in whole blood (derived from inverse of hematocrit or plasmacrit) and whole plasma with standard deviation error bars. Derived from patient #2 through #5 after PET2, PET4 and PET5. (B) Percent of ^{18}F-DCFBC activity in percent of plasma component of whole blood accounting for the whole blood activity.

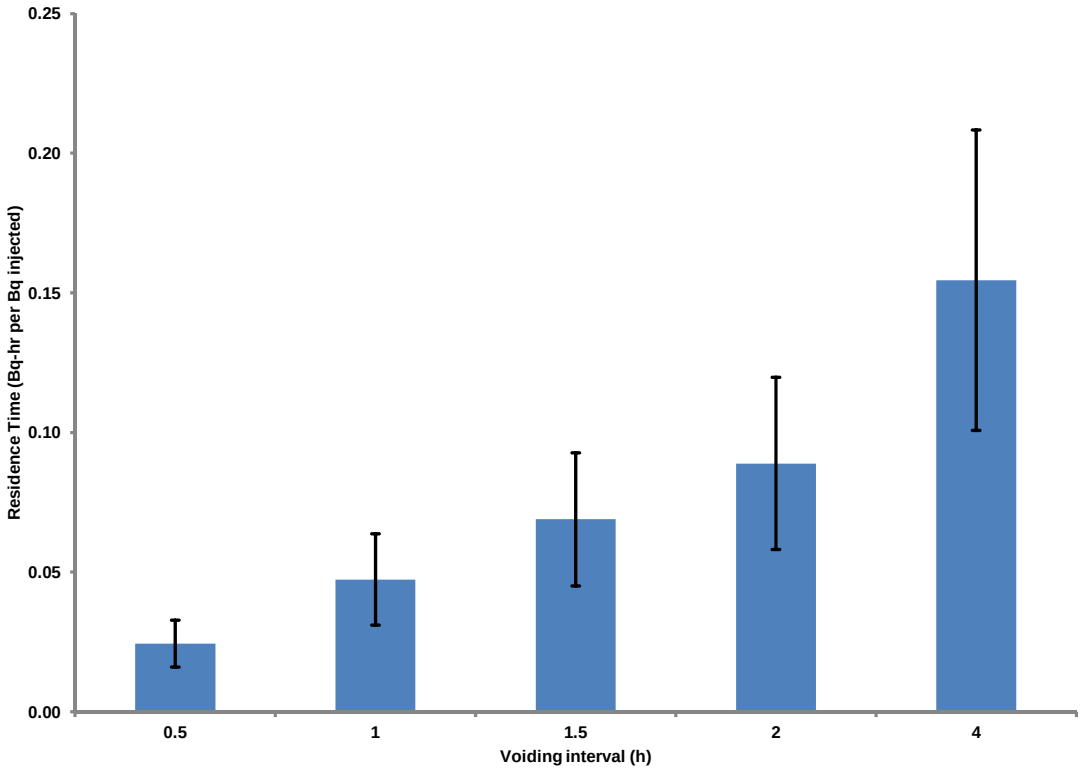

Supplemental Figure 6. Integrated time activity coefficient for the bladder contents at different voiding intervals. The voiding model of Cloutier, et al. was used to calculate the values.

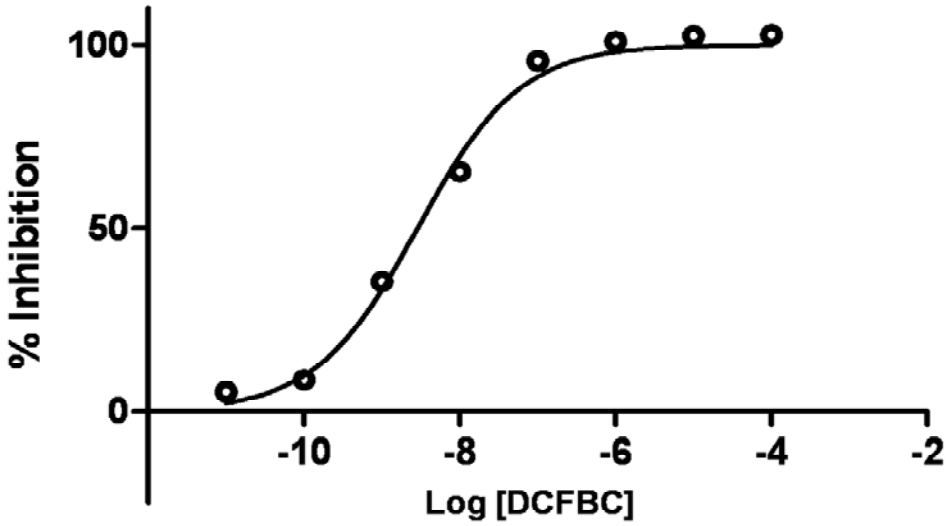

Supplemental Figure 7. DCFBC inhibits NAAG hydrolysis in normal human serum with a calculated IC_{50} of 3 nM.

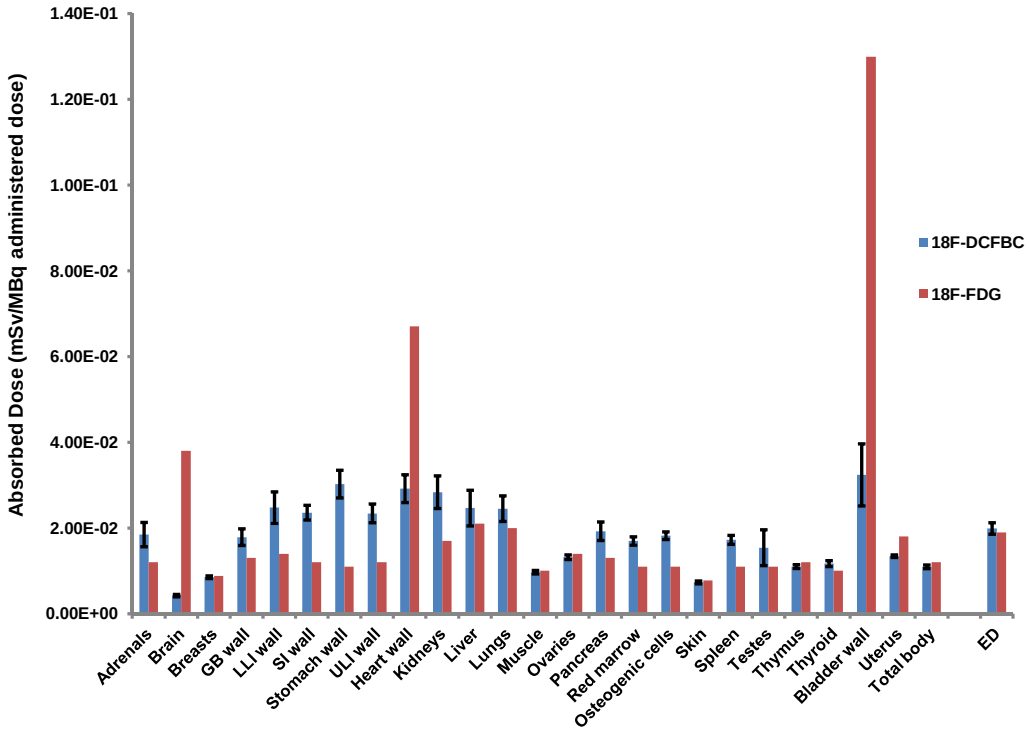

Supplemental Figure 8. Comparison of absorbed dosed for ^{18}F-DCFBCas determined from the current patient data with standard literature absorbed doses for ^{18}F FDG.